Journal of Material Sciences & Engineering

Research Article Open Access

Electrochemical Study of the Hydrogenation of $LaZr_2Cr_4Ni_5$-Based Alloys

Ines Sahli*, Mouna Elghali, Marwa Ayari, Ouassim Ghodbane and Mohieddine Abdellaoui

Laboratory of Useful Materials, National Institute for Research and Physical-Chemical Analysis, Technological Pole of Sidi Thabet, 2020 Sidi Thabet, Tunisia

Abstract

The electrochemical behavior of $LaZr_2Cr_4Ni_5$-based alloys applied as negative electrode materials for Ni–metal hydride (Ni–MH) batteries was investigated by cyclic voltammetry (CV), chronoamperometry and electrochemical impedance spectroscopy (EIS) techniques. The hydrogen diffusion coefficient, determined by CV, was equal to 1.28 × 10^{-8} cm^2s^{-1} reflecting an appropriate electrochemical hydrogenation kinetic of the $LaZr_2Cr_4Ni_5$-based compound. The evolution of the hydrogen diffusion coefficient was also investigated by EIS first at different state of charge (10% and 100%) and second as function of charge/discharge cycling. Upon the first cycle, the diffusion coefficient increases from 31.72 × 10^{-8} cm^2s^{-1} to reach a maximum value of 13.14 × 10^{-6} cm^2s^{-1} at the fifth cycle. A further cycling leads to a sharp decrease of the diffusion coefficient to 82.14 × 10^{-8} cm^2s^{-1} after 30 cycles. The hydrogen diffusion coefficient values determined by electrochemical impedance spectroscopy after 50 charge-discharge cycles are equal to 4.41.$10^{-8}$$cm^2s^{-1}$ for the α phase (10% state of charge) and 1.12 × 10^{-8} cm^2 s^{-1} for the β phase (100% state of charge). As compared to the mean value determined by cyclic voltammetry, these values are higher for α phase and less for the β phase.

The exchange current densities of the electrodes were estimated as a function of the charge/discharge cycling by EIS. The charge transfer kinetic is faster at the beginning of cycling. The chronoamperometry measurements indicate that the size of the cluster of particles involved in the electrochemical reaction (the depth or the degree of the material impregnation by the electrolyte) decreases from 63 to 6.2 µm after 50 cycles.

Keywords: Intermetallic compound; Mechanical alloying; AB_3-type compound; Hydrogen storage properties; Electrochemical measurements

Introduction

Among a series of AB_x ($0.5 \leq x \leq 5$) intermetallic compounds investigated for the reversible hydrogen storage, the AB_3-type alloys have shown promising performances as negative electrode materials for Ni-MH batteries [1-3]. They gained a great attention owing to their elevated hydrogen storage capacity of 400 $mAh.g^{-1}$ [3-7]. Comparatively to the commonly used AB_5-type alloys, the AB_3-type alloys are distinguished by their longer electrochemical stability in highly alkaline media and faster charge/discharge kinetics [2,8-10]. In our previous work [11], a novel AB_3-type $LaZr_2Cr_4Ni_5$-based alloy was successfully elaborated by mechanical alloying from $LaNi_5$ and $ZrCr_2$ precursors according to eqn. (1).

$$LaNi_5 + 2\ ZrCr_2 \rightarrow LaZr_2Cr_4Ni_5 \quad (1)$$

The as-prepared AB_3 compound crystallizes in a Rhombohedra $LaMg_2Ni_9$-type structure with R-3m space group.

The electrochemical discharge capacity determinated at ambient conditions for $LaZr_2Cr_4Ni_5$-based alloy was equal to152 $mAhg^{-1}$ and the capacity retention was 100% upon 50 charge-discharge cycles in alkaline media [11].

In our previous work [11], the hydrogen diffusion rate (D_H) values are located in the range of 10^{-8} cm^2s^{-1}. Comparatively to the literature data [5,12,13], the obtained D_H values reflect a faster kinetic of the electrochemical reaction in the $LaZr_2Cr_4Ni_5$-based materials in terms of diffusibility of hydrogen.

The aim of the present work is to investigate 1) the kinetic properties of the hydrogenation reaction such as charge transfer coefficient and hydrogen diffusion coefficient by cyclic voltametry technique, 2) the depth of the impregnation of the electrode material by the electrolyte using chronoamperometry technique and 3) the electrochemical properties of the electrolyte/electrode interface and the kinetic properties of the hydrogen storage processes by electrochemical impedance spectroscopy (EIS) measurements. The depth of the electrolyte impregnation at the electrode material during electrochemical reaction, estimated by chronoamperometry, was calculated after 50 charge/discharge cycles.

For impedance spectroscopy, the Nyquist diagrams were recorded after various charge/discharge cycles at the same states of charge (SOC).

Experimental Section

$LaZr_2Cr_4Ni_5$ alloy was prepared by mechanical alloying (MA) starting from $LaNi_5$ and $ZrCr_2$. These precursors were synthesized by ultra-high frequency (UHF) induction melting from corresponding elements (La 99.9%, Ni 99.9%, Zr 99.99%, Cr 99.99%) [11]. Briefly, the MA process was performed in a Retsh PM400 planetary ball mill with alloying condition corresponding to an injected shock power of 6.175 W/g [11,14,15]. A mixture of the $LaNi_5$ and $ZrCr_2$ powders, in a molecular ratio of 1:2, was introduced in a cylindrical steel vial (50 cm^3 in volume). The container was then loaded with five stainless steel balls (12 mm in diameter and 7.0 g in mass). The alloying duration was varied until 50 hours. After 50 h of alloying, the alloy was formed only by the AB_3 type phase, the $ZrCr_2$ precursor and the residual Cr.

***Corresponding author:** Ines Sahli, Laboratoire des Matériaux Utiles, Institut National de Recherche et d'Analyses Physico-Chimiques, Pôle Technologique de Sidi Thabet, 2020 Sidi Thabet, Tunisia, Tel: +21622591502; E-mail: sahli.ines86@yahoo.fr

Received September 19, 2019; **Accepted** November 10, 2019; **Published** November 15, 2019

Citation: Sahli I, Elghali M, Ayari M, Ghodbane O, Abdellaoui M (2019) Electrochemical Study of the Hydrogenation of $LaZr_2Cr_4Ni_5$-Based Alloys. J Material Sci Eng 8: 544.

Additionally, new peaks of low intensity, corresponding to La_2O_3 oxide, were observed upon 40 h of milling. The XRD pattern refinement of the sample obtained after 50 h of milling time is shown in Figure 1.

For the electrochemical measurements, the alloys were first grounded and sieved to less than 63 µm in a glove box under an argon atmosphere. The preparation of the working electrodes were based on the "Latex" technology and performed by mixing the active material with carbon black and PTFE in the weight ratio of 90:5:5 [16]. Two square pieces of 0.5 cm^2 of this Latex were pressed on each side of a nickel grid that constitutes the current collector and prevents the electrode plate from breaking into pieces during the charge–discharge cycling [17]. All the electrochemical measurement was performed at room temperature in a conventional three-electrode cell using a multipotentiostat- galvanostat bio-logic VMP system. The electrolyte consisted in a 1M KOH aqueous solution de-aerated by a continuous argon flow through the cell during each measurement. The counter electrode was formed by Ni oxyhydroxide $Ni(OH)_2$ and the reference electrode was Hg/HgO immersed in 1 MKOH aqueous solution [18-21]. All potentials quoted in the text are referred to this electrode. Prior to the electrochemical impedance spectroscopy measurements (EIS), the electrodes were cycled galvanostatically at C/3 and D/6 regimes of charge and discharge, respectively. Every cycle was carried out by fully charging at 150 mAg^{-1} for 3 h (C/3) up to 50% overcharge, then discharging at 75 mAg^{-1} for 6 h (D/6) at room temperature until the potential reaches the cut off voltage E=−0.6V. After 50 cycles of charge/discharge of the electrode, the cyclic voltammetry was applied between −1.3 and −0.6V vs. Hg/HgO at scan rates varying from 10 to 60 µV/s. The impedance measurements were carried out after charging the electrode at 10 and 100% of the state of charge (SOC). The frequency range was varied from 50 kHz to 1 mHz and the excitation signal was 5 mV peak-to-peak [22]. The impedance spectra were then analyzed with the ZSimplex software, used to fit the EIS spectra in order to determine the values of the components of the equivalent electric circuit of the electrolyte/electrode interface.

Results and Discussion

Cyclic voltammetry

Previous XRD measurements (Figure 1) showed that $LaNi_5$ precursor was completely consumed after 50 h of milling time. For this alloying duration, the $LaZr_2Cr_4Ni_5$ is formed with 60 wt%. Additionally, residual $ZrCr_2$ precursor is still present in the alloy with 7 wt%. New peaks of low intensity, corresponding to La_2O_3 oxide (2.35 wt%), were observed. The Cr precipitates with an amount of 30 wt% [11].

In our experimental conditions, i.e. at room temperature and atmospheric pressure, only $LaZr_2Cr_4Ni_5$ and $LaNi_5$ phases absorb hydrogen in the electrochemical reaction. However, as $LaNi_5$ phase disappeared after 50 h of milling time, the hydrogen will be absorbed only by $LaZr_2Cr_4Ni_5$phase [11]. For these reasons, all the electrochemical tests were carried out for alloy obtained after 50 h milling duration. The cyclic voltammograms (CVs) of $LaZr_2Cr_4Ni_5$-based electrodes, recorded at different scan rates, are shown in Figure 2. The CV curves were recorded after 50 charge/discharge cycles. The cathodic scan shows the beginning of the hydrogen reduction (absorption reaction) at about -0.85 V followed by a continuous decrease of the cathodic potential until -1.1 V. The absorbed hydrogen atoms diffuse in the interstitial sites of the alloy lattice [18,23]. When the potential is reversed to the opposite direction, the current increases and an anodic peak was observed for positive current. This peak corresponds to the oxidation (desorption) of the hydrogen atoms absorbed previously during the charge sweep.

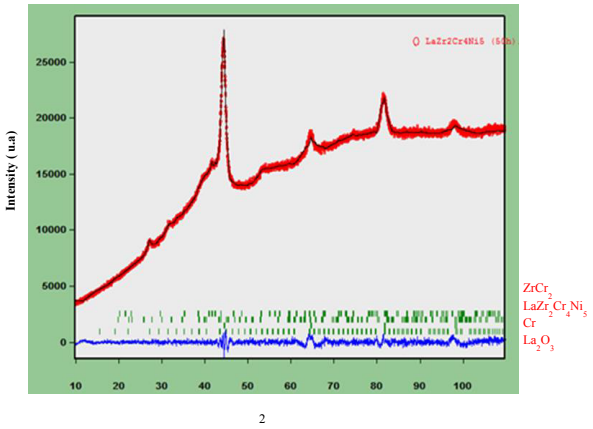

Figure 1: Rietveld refinement of the X-ray diffraction pattern of the sample obtained after 50 h of mechanical alloying.

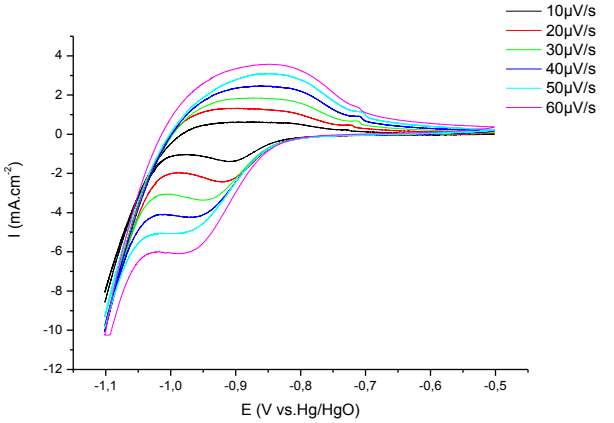

Figure 2: Cyclic voltammograms of the $LaZr_2Cr_4Ni_5$ -based electrode obtained at potential scan rates ranging between 10 and 60 µV/s.

Figure 3a shows that the potential value of the anodic peak (E_{ap}), corresponding to the maximum current value, is linearly dependent on log (ϑ) while Figure 3b shows that the value of the anodic current varies linearly with the square root of the scan rate ($\vartheta^{1/2}$). This behavior of potential and current variations corresponds to a semi-infinite and irreversible system [18]. In this case, the potential oxidation peak value (E_{ap}) and the current oxidation peak value (I_{ap}) are given according to the following equations [18,24,25]:

$$\frac{dE_{ap}}{dlog(\vartheta)} = \frac{2.3RT}{\alpha nF} \quad (2)$$

where R is the constant of rare gas, T the temperature of the electrochemical cell, α the charge transfer coefficient, n the number of exchanged electrons and F the Faraday constant.

$$I_{ap} = 0.496\alpha^{1/2}(nF)^{3/2} SC_o(\frac{\vartheta D}{RT})^{1/2} \quad (3)$$

where S is the geometric surface of the electrode (cm^2), C_o the concentration of diffusion species ($mol.cm^{-2}$) and D the hydrogen diffusion coefficient ($cm^2.s^{-1}$).

So, the values of the charge-transfer coefficient (α) and the hydrogen diffusion coefficient (D_H) of $LaZr_2Cr_4Ni_5$-based alloy are

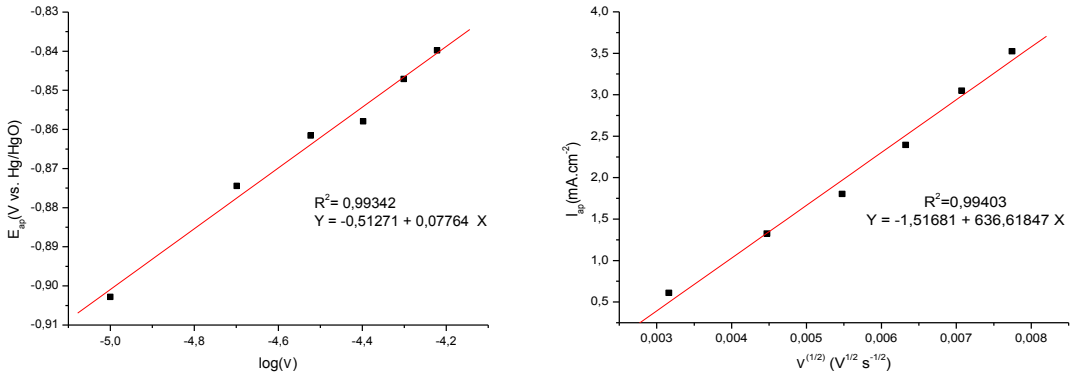

(a) (b)

Figure 3: a) Variation of E_{ap} as function of log (ϑ) and b) I_{ap} as function of square root of potential scan rate (ϑ).

calculated respectively from the slope of the curves E_{ap}=f (log (ϑ)) and I_{ap}=f ($\vartheta^{1/2}$) [11]. The hydrogen diffusion coefficient (D_H) value is equal to 1.28 × 10^{-8} cm^2 s^{-1}. Comparatively to the literature data (Table 1), the D_H value of $LaZr_2Cr_4Ni_5$-based alloy reflects a faster kinetic for the electrochemical reaction in terms of diffusibility of hydrogen.

The charge transfer coefficient is equal to 0.38 ranges between 0.3 and 0.7 and can be approximated to 0.5, suggesting that the charge and discharge reactions are reversible and the system presents the same tendency for the charge and the discharge processes [24,26].

Chronoamperometry

Figure 4 shows the variation of the semilogarithmic discharge current log(i) versus time for $LaZr_2Cr_4Ni_5$-based alloy.

When we assume that the hydride alloy particles have a spherical form [18-29], the diffusion of hydrogen in the bulk of these particles can be given, in the spherical coordinate, by the following equation (4) as:

$$\frac{\partial(rC)}{\partial t} = \bar{D}\frac{\partial^2(rC)}{\partial r^2} \quad (4)$$

where t is the time, c is the hydrogen concentration in the alloy, $\bar{D}$ is the average diffusion coefficient of hydrogen in the bulk and r is the distance from the center of the sphere.

Eqn. (5) gives the solution of the diffusion equation given by Crank as indicated by Weixiang [30], under different boundaries, as:

$$\frac{C-C_0}{C_s-C_0} = 1+\frac{2a}{\pi r}\sum_{n=1}^{\infty}\frac{(-1)^n}{n}sin\frac{n\pi r}{a}\exp\left(-\frac{\bar{D}n^2\pi^2 t}{a^2}\right) \quad (5)$$

where C_0 and Cs are, respectively, the initial hydrogen concentration in the bulk material and the hydrogen concentration in the surface of the alloy and a is the sphere radius and. So, the diffusion current will vary with the time according to eqn. (6):

$$i = \pm\frac{6F\bar{D}}{da^2}(C-Co)\sum_{n=1}^{\infty}\exp(-\frac{n^2\pi^2 Dt}{a^2}) \quad (6)$$

where, F is the Faraday constant and d the density of material.

For a long time, eqn. (6) can be rewritten as follows:

$$log(i) = log\left[\pm\frac{6F\bar{D}}{da^2}(Co-Cs)\right]-\frac{\pi^2\bar{D}}{2.303a^2}t \quad (7)$$

Compound	Diffusion coefficient *D* (×10^{-10} cm^2 s^{-1})	Ref.
$LaZr_2Cr_4Ni_5$	128	This work
$LaTi_2Cr_4Ni_5$	717	[12]
$CeZr_2Cr_4Ni_5$	200	[27]
$La_{1.6}Mg_{1.4}Ni_9$	9.0	[28]
$La_{2.2}Mg_{0.8}Ni_9$	2.4	[28]
La_2MgNi_9	7.1	[29]
$La_2Mg(Ni_{0.95}Al_{0.05})_9$	1.2	[5]
$La_2Mg(Ni_{0.95}Co_{0.05})_9$	1.5	[5]
$La_2Mg(Ni_{0.95}Sn_{0.05})_9$	7.6	[5]

Table 1: Summary of literature data on electrochemical performances of AB_3-type intermetallic alloys.

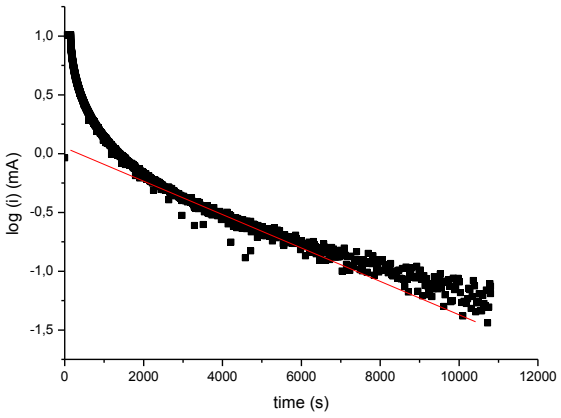

Figure 4: Variation of the diffusion current as a function of time recorded after 50 charge-discharge cycles for the $LaZr_2Cr_4Ni_5$– based electrode.

The ± sign in eqns. (6) and (7) indicates the charge state for the minus sign and the discharge state for the plus sign. According to eqn. (7), $\frac{\bar{D}}{a^2}$ can be evaluated from the slope of the plot of log(i) versus time t. Taking into account that the value of the hydrogen diffusion coefficient D is determined by the cyclic voltammetry, the radius "a" of the particles involved in the electrochemical reaction for each alloy (supposed as spherical shaped), can be calculated from the value the slope $\frac{\bar{D}}{a^2}$ of the corresponding chronoamperogramms.

The plot can be divided into two regions: for t<2000 s, the current decreases rapidly under a charge–transfer control [19]. For t>2000 s, the diffusion current decreases linearly with time. The average radius of individual or agglomerated material, involved in the electrochemical reaction, are calculated from the slope of I=f(t) for t >2000 s (Table 1) [19].

XRD characterization shows that the synthesized material is nanostructured with a diffraction crystallite size ranging from 7 to 5 nm [11]. Nevertheless, SEM micrographs show that nanoparticles are agglomerated in micrometric clusters [11]. Prior to the charge/discharge process, the alloy powder was ground mechanically and was saved to less than 63 µm in a glove box for the preparation of the negative electrode.

The calculated radius (a) of material involved the electrochemical reaction after 50 charge–discharge cycles, is equal to 6.2 µm. So, chronoamperometry measurements can inform on the depth degree of the electrolyte penetration and if it can reach the nanometer scale of the material or it surround only the micrometer clusters. Hence, it is assumed that 1) the electrolyte cannot penetrate until the nanometer scale and it surrounds only micrometric clusters and 2) the micrometric clusters size decreases during the hydrogen absorption/desorption processes from 63 to 6.2 µm. This decrease is assumed to be due to the pulverization of powders induced by the expansion of the lattice volume (Table 2) [18,31].

EIS measurements

The (EIS) measurements are performed to investigate the kinetics of hydrogen diffusion in $LaZr_2Cr_4Ni_5$-based alloys. Typical Nyquist diagrams are reported in Figure 5 for 100% state of charge (SOC) after 30 charge-discharge cycles for the $LaZr_2Cr_4Ni_5$ compound obtained after 50 h of mechanical alloying. The observed spectra (Figure 5) can be divided into three regions: a small semicircle in the high frequency region (50 Hz–50 kHz). The diameter of the high frequency semicircle corresponds to the charge transfer resistance (R_{tc}) of the interface between the material and the electrolyte. The maximum value of frequency of this semicircle allows the calculation of the double layer capacity as C_{dl}=943,13 µF.

The slope of about 45° in the medium frequency range (4–50 Hz) allows the calculation of the Warburg impedance which depends on the diffusion phenomenon of hydrogen in the material. The radius of the semicircle at low frequency (1 mHz–4 Hz) gives the resistance of particles in the bulk of the material. It exhibits marked dependence on the cycle number.

Table 3 summarizes the values of parameters determined by the fitting of Nyquist plots. The fit accuracy is confirmed by the χ^2 value lower than 5.10^{-3} [32].

High frequencies region: At high frequencies region, the small semicircle characterizes the electrical properties of the double layer (C_{dl}) which materialize the interface between the electrolyte and the material. It give the charge transfer resistance (R_{ct}) and the capacity (C_{dl}) of the double layer [33-35]. Table 3 gives the charger transfer resistance R_{ct}, the capacity of the double layer C_{dl}, the electrolyte resistance R_e and the exchange current density I_0 for $LaZr_2Cr_4Ni_5$ sample at 100% SOC during the cycling process. The exchange current density I_0 and the double layer capacity C_{dl} are calculated as follows:

$$I_0 = \frac{RT}{nFSR_{ct}} \quad (8)$$

$$C_{dl} = \frac{1}{2\pi f^* R_{ct}} \quad (9)$$

where n is the number of the exchanged electrons, T is the working temperature, F is the Faraday constant, S is the geometric area of the electrode, f* is the proper frequency and R_{ct} is the charger transfer resistance.

The electrolyte resistance values (R_e) are independent of the cycle number. The R_{ct} value (Table 3) decreases initially from 2 Ω (1st cycle) to 0.43 Ω (10th cycle). This result suggests that the hydrogen diffusion reaction at the electrode surface is more efficient in the first 10 cycles, which can be attributed to the generation of new active surface sites with high electrocatalytic activity during the activation of the alloy. So, the phenomena of the charger–transfer begin more easy when the material is activated [36]. While the double layer capacitance (C_{dl}) increases gradually from 398,83 µF at the first cycle to until 943,13 µF

Milling time (h)	C_0 (mol cm^{-3})	α	D_H (cm^{2}s^{-1})	a (µm)
50	0.034	0.38	1.28×10^{-8}	6.2

Table 2: Values of α, D_H and "a" of $LaZr_2Cr_4Ni_5$-based electrodes.

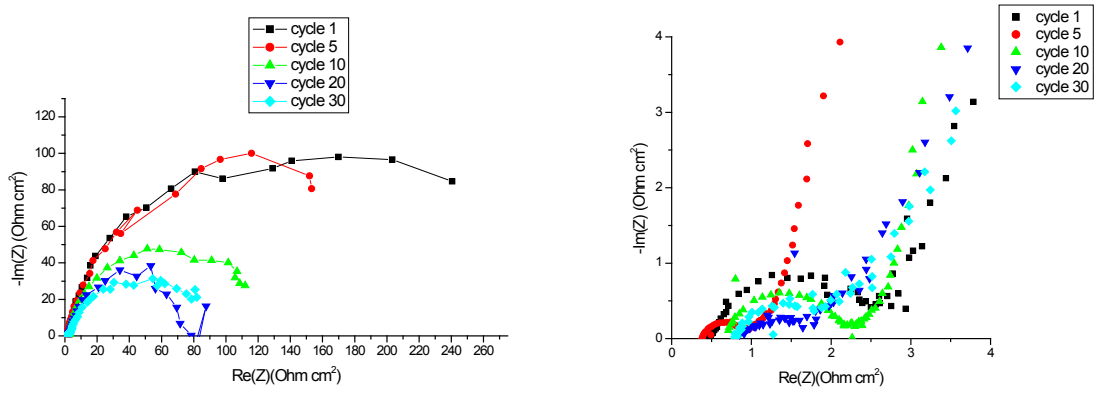

Figure 5: a) Typical Nyquist plots for the $LaZr_2Cr_4Ni_5$ (50 h) electrode at 100% state of charge during the first 30 cycles of charge/discharge and b) Enlarged view of the high frequency region.

at 30th cycle and then decreases to 422.62 µF at 50th cycle showing an irregular trend due to pulverization [36].

After further cycling, the R_{ct} value increases to 5.02Ω (50th cycle). In fact, the reaction of hydrogen at the surface tends to become less efficient due to the surface passivation by the formation of a hydroxide film at the alloy surface [37].

The exchange current density (I_0) is a powerful parameter for measuring the kinetic of the electrochemical hydrogenation [38,39]. The value of I_0 increases from 13.79 $mAcm^{-2}$ and reached its maximum of 67.66 $mAcm^{-2}$ after 10 cycles. A further cycling leads to a decrease of I_0, which again indicates a capacity fading as hydrogen diffusion is becoming less efficient. The variation of R_{ct} and I_0 as a function of the cycle number shows that the charge transfer kinetics is better at the beginning of cycling (Table 3).

Warburg region: The Warburg region is represented by a 45° straight line variation of Im(Z) as function of Re(Z) in the medium frequency range (4-50 Hz). Under semi-infinite diffusion conditions, the apparent chemical diffusion coefficient of hydrogen (D_H) can be calculated from Warburg's prefactor A_W (slope of the plot Re(Z) versus $w^{-1/2}$ (Figure 6), where w=2πf) as follows [40]:

$$A_W = \frac{Vm}{nFS\sqrt{2DH}}\left(\frac{dE}{dX}\right) \quad (10)$$

where Vm is the molar volume of the alloy, $\frac{dE}{dX}$ is the slope of the electrochemical discharge isotherm at each X value, F is the Faraday constant and S is the geometric area (1 cm^2 in this work). The variations of A_W and D_H during cycling are given in Table 3. According to our previous study [11], $LaZr_2Cr_4Ni_5$-based alloy is easily activated after several charge and discharge cycles. As a consequence of the decripitation process occurred during the first cycles of absorption/desorption of the hydrogen, the number of vacant sites increases and, consequently, the diffusion of hydrogen becomes faster [11]. The hydrogen diffusion coefficient (D_H) is found to increase from 31.7×10^{-8} cm^2s^{-1} at the first cycle to 13.14×10^{-6} cm^2s^{-1} after 5 cycles. By increasing the number of cycles, the values of the hydrogen diffusion coefficient in the bulk material of $LaZr_2Cr_4Ni_5$ decreases sharply to 1.12×10^{-8} cm^2s^{-1} after 50 cycles.

Figure 7 shows the electrochemical impedance spectra of the $LaZr_2Cr_4Ni_5$ electrode after activation during 50 cycles at 10% and 100% states of charge.

The 10% state of charge corresponds to the solid solution α phase whereas the 100% state of charge belongs to the hydride β phase. The hydrogen diffusion coefficient D_H values are higher for the α phase and lower for the β phase. The D_H value determined by the cyclic voltammetry is located between those corresponding to 10% and 100% states of charge. It represents a mean value. We assume that the value of the hydrogen diffusion coefficient depends on the hydrogen content in the alloy in a way that it decreases when the state of charge increases. In fact, in the α phase, the number of interstitial sites susceptible to accept the hydrogen atoms is more numerous and consequently the hydrogen diffuses easily. So, the D_H is higher. However, in the β phase, the interstitial sites are almost saturated and the hydrogen diffuses hardly. So, D_H is lower. The value given by the cyclic voltammetry represents a medium value representing a medium state. So, it will be lower than that corresponding to the α phase and higher than that corresponding to the β phase. The values of D_H determined by EIS are in good agreement with those reported in the literature [17].

During the charge/discharge cycling, rare earth elements, such

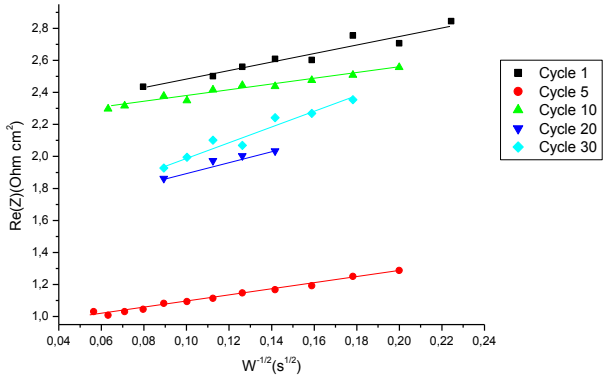

Figure 6: Variation of Z_{real} Vs $W^{-1/2}$ of $LaZr_2Cr_4Ni_5$ in the Warburg region at 100% state of charge during the first 30 cycles.

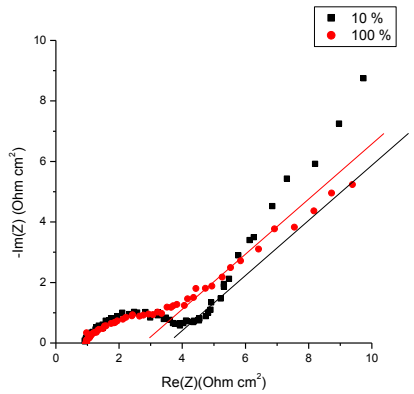

Figure 7: Variation of the Nyquist plot for 10 and 100% state of charge after activation during 50 cycles.

Cycle number	SOC	R_e (Ω)	R_{ct} (Ω)	C_{dl} (µF)	R_{LF} (Ω)	I_0 ($mAcm^{-2}$)	A_w	D ($10^{-6}cm^2s^{-1}$)	χ^2 (10^{-3})
1	100%	0.49	2.00	398.83	196.6	13.79	2.75	0.31	1.85.
5	100%	0.67	1.41	182.44	111.6	19.99	1.91	13.14	3.24
10	100%	0.40	0.43	28.41	232.7	67.66	1.79	10.06	2.51
20	100%	0.83	0.84	473.98	72.6	30.81	3.28	1.09	2.29
30	100%	0.81	0.85	943.13	87.6	37.31	4.73	0.82	1.52
50	10%	0.44	4.81	374.85	86.1	5.78	26.51	0.04	1.32
	100%	0.48	5.02	422.62	85.5	5.21	31.33	0.01	0.65

Table 3: Kinetic parameters of the $LaZr_2Cr_4Ni_5$ (50 h) electr.

as La, segregate to the grain boundaries where they were subjected to the corrosion in alkaline electrolytes [17]. The corrosion products are deposited on the surface of the grain particles as needle-shaped $La(OH)_3$. This corrosion leads to an increase in resistance between the alloy grains, which in turn may affects the kinetic properties [17]. Several authors assumed that the oxygen penetration depth in the surface layers of the alloys increased with increasing charging cycles [17]. So, the penetration of oxygen into the surface layers leads to an easy oxidation of metallic elements during the charging and discharging process. Such an oxidation phenomenon leads to a limitation of the hydrogen diffusion from the surface to the bulk of the alloy [17]. Heng et al. [41] reported that when the oxide film or corrosion layer is formed on the surface of the alloy particles, the reaction rate should be influenced more or less by this surface layer. Consequently, it was suggested that the corrosion phenomenon may affects the kinetic properties and leads to a decrease of the hydrogen diffusion coefficient in the material.

Low frequencies region: The larger semicircle in the low frequency region (LF) corresponds to the resistance of the particles in the bulk of the alloy [35]. The diameter of this large semicircle significantly decreases upon increasing the cycle number. For $LaZr_2Cr_4Ni_5$, this resistance (R_{LF}) decreases from 196.6 Ω at the first cycle to 85.5 Ω after 50 cycles. We assume that the decrease of the particle size from 63 to 6.2 μm, occurred during the decripitation of powder upon hydrogen absorption/desorption processes [18,32], increases the contact between the particles and then reduces the R_{LF} value. This is reflected by the reduction of the diameter of the semicircle. Nevertheless, it has been suggested that this resistance is attributed to the oxide/hydroxide film formed on the surface, which reduces the electrochemical catalytic activity of the electrode surface [36]. During repetitive charge–discharge cycling, the layer thickness becomes active and causes a decrease in the resistance.

Conclusion

In this work, the electrochemical properties of a novel AB_3-type-rich alloy, consisting in $LaZr_2Cr_4Ni_5$-based materials were investigated. The value of the hydrogen diffusion coefficient estimated after 50 cycles by cyclic voltammetry is equal to 1.28×10^{-8} cm^2 s^{-1}, reflecting a good absorption/desorption kinetic and a high hydrogen diffusivity through the $LaZr_2Cr_4Ni_5$-rich alloy. The effective value of the diffusion coefficient of hydrogen estimated by EIS through $LaZr_2Cr_4Ni_5$ electrode at 10 and 100% SOC determined after 50 cycles are, respectively, equal to 4.41 and $1.12 \times 10^{-8}$$cm^2$ s^{-1}. The exchange current densities of MH electrodes were estimated by EIS as a function of cycling. The charge transfer kinetics is much better at the beginning of cycling, where the electrode is electrochemically activated.

References

1. Latroche M, Percheron-Guégan A (2003) Structural and thermodynamic studies of some hydride forming RM_3-type compounds (R=lanthanide, M=transition metal). J Alloy Compd 356: 461-468.
2. Kadir K, Sakai T(2003) Structural investigation and hydrogen storage capacity of $LaMg_2Ni_9$ and $(La_{0.65}Ca_{0.35})(Mg_{1.32}Ca_{0.68})Ni_9$ of the AB_2C type structure. J Alloy Compd 302: 112-117.
3. Chen J, Takeshita HT, Tanaka H , Kuriyama N, Sakai T, et al. (2000) Hydriding properties of $LaNi_3$ and $CaNi_3$ and their substitutes with $PuNi_3$-type structure. J Alloy Compd 302: 304-313.
4. Liao B, Lei YQ, Chen LX, Lu GL, Pan HG, et al. (2006) The structural and electrochemical properties of $La_2Mg(Ni_{0.8-x}Co_{0.2}Al_x)_9$ (x=0-0.03) hydrogen storage electrode alloys. J Alloy Compd 415:239-43.
5. Liao B, Lei YQ, Chen LX, Lu GL, Pan HG, et al. (2004) A study on the structure and electrochemical properties of $La_2Mg(Ni_{0.95}M_{0.05})_9$ (M=Co, Mn, Fe, Al, Cu, Sn) hydrogen storage electrode alloys. J Alloy Compd 376:186-195.
6. Kadir K, Kuriyama N, Sakai T, Ueharaa I, Eriksson L (1999) Structural investigation and hydrogen capacity of $CaMg_2Ni_9$: A new phase in the AB_2C_9 system isostructural with $LaMg_2Ni_9$. J Alloy Compd 284:145-54.
7. Kadir K, Sakai T, Uehara I (1999) Structural investigation and hydrogen capacity of YMg_2Ni_9 and $(Y_{0.5}Ca_{0.5})(MgCa)$ Ni_9: new phases in the AB_2C_9 system isostructural with $LaMg_2Ni_9$. J Alloy Compd 287: 264-70.
8. Pan HG, Liu YF, Gao MX, Lei YQ, Wang QD (2005) Electrochemical Properties of the $La_{0.7}Mg_{0.3}Ni_{2.65-x}Mn_{0.1}Co_{0.75}Al_x$ (x=0-0.5) Hydrogen Storage Alloy Electrodes. J Electrochem Soc 152: 326–332.
9. Kadir K, Sakai T, Uehara I (1997) Synthesis and structure determination of a new series of hydrogen storage alloys; RMg_2Ni_9 (R=La, Ce, Pr, Nd, Sm and Gd) built from $MgNi_2$ Laves-type layers alternating with AB_5 layers. J Alloy Compd 257:115-21.
10. Elghali M, Abdellaoui M, Paul-Boncour V, Latroche M (2013) Synthesis and structural characterization of mechanically alloyed AB_3-type based material: $LaZr_2Mn_4Ni_5$. Intermetallics 41: 76-81.
11. Sahli I, Ghodbane O, Abdellaoui M (2016) Elaboration and electrochemical characterizationof $LaZr_2Cr_4Ni_5$-based metal hydride alloys. Ionics 22: 1973-1983.
12. Ayari M, Ghodbane O, Abdellaoui M (2015) Elaboration and electrochemical characterization of $LaTi_2Cr_4Ni_5$-based metal hydride alloys. Int J Hydrogen Energy 40: 10934 -10942.
13. Chebaba S, Abdellaouia M, Latrocheb M, Paul-Boncourb V (2016) LaCaMgNi9 synthesized by mechanical alloying: Structural and electrochemical characterization. Journal of the Tunisian Chemical Society 18: 52-59.
14. Abdellaoui M, Gaffet E (1995) The physics of mechanical alloying in a planetary ball mill: Mathematical treatment. Acta Metal Mater 43: 1087-1098.
15. Abdellaoui M, Gaffet E (1994) A mathematical and experimental dynamical phase diagram for ballmilled $Ni_{10}Zr_7$. J Alloy Compd 209: 351-361.
16. Mathlouthi H, Lamloumi J, Latroche M, Percheron Guégan A (1999), Study of polysubstituted intermetallic hydrides electrochemical applications. Ann Chim Sci Matter 22: 241-244.
17. Ben Moussa M, Abdellaoui M, Mathlouthi H, Lamloumi J, Percheron Guégan A (2005) Electrochemical properties of the $MmNi_{3.55}Mn_{0.4}Al_{0.3}Co_{0.4}Fe_{0.35}$ compound. J Alloys Compd 400: 239-244.
18. Ben Moussa M, Abdellaoui M, Mathlouthi H, Lamloumi J, Percheron Guégan A (2006) Investigation of the cycle stability and diffusivity of hydrogen in the $MmNi_{3.55}Mn_{0.4}Al_{0.3}Co_{0.6}Fe_{0.15}$ compound. J Alloys Compd 407: 256-262.
19. Mathlouthi H, Khaldi C, Ben Moussa M, Lamloumi J, Percheron-Guégan A (2004) Electrochemical study of mono-substituted and poly-substituted intermetallic hydrides. J Alloys Compd 375: 297-304.
20. Belgacem YB, Khaldi C, Lamloumi J, Takenouti H (2015) Effect of the discharge rate on the electrochemical properties of LaY_2Ni_9 hydrogen storage alloy. J Alloy Compd 631: 7-14.
21. Ben Fradj A, Ben Moussa M, Abdellaoui M, Lamloumi J (2015) Study of Structural, Thermodynamic and Electrochemical Properties of $MmNi_{3.55}Mn_{0.4}Al_{0.3}Co_{0.75-x}Fe_x$ (x=0 and 0.75) Compounds. Am J Ener Power Engin 2: 79-91.
22. Ben Moussa M, Abdellaoui M, Khaldi C, Mathlouthi H, Lamloumi J, et al. (2005) Effect of substitution of Mm for La on the electrochemical properties of the $LaNi_{3.55}Mn_{0.4}Al_{0.3}Co_{0.75}$ compound. J Alloy Compd 399: 264-269.
23. Ben Moussa M, Abdellaoui M, Mathlouthi H, Lamloumi J, Percheron-Guégan A (2008) Electrochemical properties ofthe $MmNi_{3.55}Mn_{0.4}Al_{0.3}Co_{0.75-x}Fe_x$ (x=0.55 and 0.75) compounds. J Alloy Compd 458:410-414.
24. Herr T, Noack J, Fischer P, Tübke J (2013) 1,3-Dioxolane, tetrahydrofuran, acetylacetone and dimethyl sulfoxideas solvents for nonaqueous vanadium acetylacetonateredox-flow-batteries. Electrochem Acta 113:127-133.
25. Bard A, Faulkner L (1983) Principes, Methodes et Applications. Paris: Masson éditeur p: 791.
26. Bard A, Faulkner L (1983) Principes, Methodes et Applications. Masson éditeur, Paris p: 791.
27. Sahli I, Ghodbane O, Abdellaoui M (2017) Electrochemical hydrogenation of $CeZr_2Cr_4Ni_5$ based alloys. Materials Research Bulletin 85 10-17.

28. Liao B, Lei YQ, Chena LX, Lub GL, Pan HG, et al. (2004) Effect of the La/Mg ratio on the structure and electrochemical properties of $La_xMg_{3-x}Ni_9$ (x=1.6–2.2) hydrogen storage electrode alloys for nickel-metal hydride batteries. J Power Sources 129:358–367.

29. Liao B, Lei YQ, Chen LX, Lu GL, Pan HG, et al. (2004) Effect of Co substitution for Ni on the structural and electrochemical properties of $La_2Mg(Ni_{1-x}Co_x)_9$ (x=0.1–0.5) hydrogen storage electrode alloys. Electrochim Acta 50:1057–1063.

30. Weixiang C (2000) Cyclic voltammetry and electrochemical impedance of $MmNi_{3.6}Co_{0.7}Mn_{0.4}Al_{0.3}$ alloy electrode before and after treatment with a hot alkaline solution containing reducing agent. J Power Sources 90:201–205.

31. Geng M, Han JW, Feng F, Northwood DO (1999) Charging/ Discharging Stability of a Metal Hydride Battery Electrode. J Electrochem Soc 146: 2371–2375.

32. Castro EB, Real SG, Bonesi A, Visintin A, Triaca WE (2004) Electrochemical impedance characterization of porous metal hydride electrodes. Electrochemica acta 49: 3879-3890.

33. Kuriyama N, Sakai T, Miyamura H, Uehara I, Ishikawa H (1993) Electrochemical impedance and deterioration behavior of metal hydride electrodes. J Alloys Compd 202: 183-197.

34. Zhang W, Kumar MP, Srinivasan S, Ploehn HJ (1995) AC Impedance Studies on Metal Hydride Electrodes. J Electrochem Soc 142: 2935-2943.

35. Zhanga Y, Yanga T, Shanga H, Chena L, Ren H, et al. (2012) Electrochemical Hydrogen Storage Kinetics of $La_{0.75-x}$ $ZrxMg_{0.25}Ni_{3.2}Co_{0.2}Al_{0.1}$ (x=0-0.2) Alloys Prepared by Melt Spinning. Energy Procedia 16: 1275–1282.

36. Ben Moussa M, Abdellaoui M, Mathlouthi H, Lamloumi J, Percheron-Guégan A (2013) Investigation on the structure, thermodynamic and electrochemical properties of the $MmNi_{3.55}Mn_{0.4}Al_{0.3}Fe_{0.75}$ compound used as negative electrode in Ni-MH batteries. J Alloy Compd 575:414–418.

37. Raju M, Manimaran k, Ananth MV, Renganathan NG (2007) An EIS study on the capacity fades in $MmNi_{3.6}Al_{0.4}Mn_{0.3}Co_{0.7}$ metal-hydride electrodes. Int Jo Hydrogen Energy 32: 1721 – 1727.

38. Yuan H, Kuroki K, Hirakawa K, Tomokiyo A (1984) Electrode resistance of metal hydride in alkaline aqueous solution. Jpn J Appl Phys 23: 1619–1623.

39. Notten PHL, Hokkeling P (1991) Double-Phase Hydride Forming Compounds: A New Class of Highly Electrocatalytic Materials. J Electrochem Soc 138: 1877–1885.

40. Khaldi C, Mathlouthi h, Lamloumi J, Percheron-Guégan A (2004) Electrochemical impedance spectroscopy and constant potential discharge studies of $LaNi_{3.55}Mn_{0.4}Al_{0.3}Co_{0.75-x}Fe_x$ hydrides alloy electrodes. J Alloys Compd 384: 249–253.

41. Yang H, Chen Y, Tao M, Wu C, Shao J, et al. (2010) Low temperature electrochemical properties of $LaNi_{4.6-x}Mn_{0.4}M_x$ (M=Fe or Co) and effect of oxide layer on EIS responses in metal hydride electrodes. Electrochim Acta 55: 648–655.